Electronic Supplementary Material (ESI) for New Journal of Chemistry.

The Fabrication of BSA@PB-P Nanoparticle and its Drug Loading and Controlled Release of Lamivudine

Yan Zhao[b]*†, Jing-Jing Zhao[c]†, Yi-Ran Yao[a], Yang Yang[a]*

[a] School of Chemical Engineering and Technology, Hebei University of Technology, Tianjin, 300130, P. R. China

[b] Department of Endocrinology, The Second Hospital of Tianjin Medical University, Tianjin, 300211, P. R. China

[c] Department of Nephrology, The Second Hospital of Tianjin Medical University, Tianjin, 300211, P. R. China

[†] These authors contributed equally to this work.

*Corresponding author: yangyang0410@hebut.edu.cn

zhaoyan@tmu.edu.cn

Experimental Section

Materials. All the chemicals were reagent-grade using in this study. BSA was purchased from Beijing Dingguo Biotechnology Co. Ltd. $K_3[Fe(CN)_6]$, polyvinyl pyrrolidone (PVP), hydrochloric acid, and lamivudine (LAM) were obtained from Shanghai Aladdin Reagent Co. Ltd. Ultrapure water throughout all experiments were supported by Hangzhou Wahaha Group Co. Ltd. All chemical reagents were analytically pure. Dialysis tube was regenerated cellulose and purchased from Shanghai yuanye Bio-Technology Co., Ltd, and the interception range of molecular weight was 8,000-14,000.

Instruments. UV/Vis spectra were recorded in a conventional quartz cell (light path 10 mm) by METASH UV-6100 instruments. The samples for SEM measurements were prepared by dropping each sample solution onto a coverslip followed by evaporation of the solvent at room temperature. SEM experiments were performed on FEI Nova Nano SEM450 scanning electron microscope. Transmission electron microscope (TEM) images were obtained on FEI Talos F200S microscope instrument with an accelerating voltage of 200 kV. The samples were prepared by placing a drop of solution (1 mg mL^{-1}) on a carbon-coated copper grid and air-dried. The sample solutions for DLS experiments were prepared by filtering each solution through a 450 nm syringe-driven filter (JET BIOFIL) into a clean scintillation vial. The samples were examined on Nano-ZS90 (Malwern Company) at 25 °C. All DLS measurements were performed at the scattering angle of 90°. X-ray diffraction (XRD) analysis was carried out on Germany Bruker D8 Discover. X-ray photoelectron spectroscopy (XPS) was performed on

Thermo Fisher ESCALAB 250Xi.

Synthesis of PB-S. The solid prussian blue nanoMOF (**PB-S**) was prepared according to the modified method in the reported literature [1]. Briefly as follows, PVP (3 g) and $K_3[Fe(CN)_6]$ (113.14 mg) was dissolved in 0.01 M HCl (40 mL), and the mixture was stirred at room temperature for 30 min. Then the mixed solution was transferred to a Teflon-lined autoclave and reacted at 80 °C for 20 h. The product **PB-S** was collected by centrifugation for 10,270 g for 15 min, and then washed for three times by deionized water and ethanol, respectively. Finally, the **PB-S** nanoparticles were dried at room temperature for 12 h and obtained as dark blue powder.

Synthesis of PB-P. PB-S (20 mg) and PVP (100 mg) were dissolved in 1 M HCl (20 mL), and the mixture was stirred at room temperature for 2 h. Then the mixed solution was transferred to a Teflon-lined autoclave and reacted at 140 °C for 2, 2.5 and 3 h, respectively. After centrifugation, the residue was washed for three times by deionized water and ethanol, respectively, and the **PB-P** nanoparticles by different etching time were obtained as dark blue powder.

Preparation of BSA@PB-P. BSA (6 mg) in 1 mL deionized water was added into the aqueous solution containing **PB-P** (1 mg mL^{-1}, 1 mL) under ultrasonic condition (ultrasonic bath, 100 W, 19 °C) for 6 h. The suspension was centrifuged at 10,270 g for 20 min, and washed by deionized water once to obtain the dispersed solution of **BSA@PB-P**.

Preparation of BSA@PB-P@LAM. LAM with 4 mg, 6 mg, 8 mg, 10 mg, and 12 mg was respectively dissolved in 2 mL deionized water, and then 1 mL **PB-P** nanoparticle

solution with 1 mg mL^{-1} was added and the mixture was stirred (300 rpm) for 4 h in dark at r.t.. Then 6 mg BSA in 1 mL deionized water was added and continuously stirred (300 rpm) for overnight at r.t.. Finally, the obtained **BSA@PB-P@LAM** nanoparticles were centrifuged (10,270 g, 20 min) and washed twice by deionized water. The encapsulation rate (ER) and loading rate (LR) were calculated by the following equations:

$$ER\ (\%) = \frac{m\ (LAM)'}{m\ (LAM)} * 100\%$$

$$LR\ (\%) = \frac{m\ (LAM)'}{m\ (LAM)' + m\ (MOF)} * 100\%$$

where m (LAM)' was the mass of loaded LAM, m (LAM) was the mass of feeding LAM, m (MOF) was the mass of **BSA@PB-P** nanoparticles.

LAM release from BSA@PB-P@LAM *in vitro*. LAM solution and **BSA@PB-P@LAM** nanoparticles were dispersed in 2 mL deionized water and put into dialysis tube. Then the dialysis devices were respectively placed in beakers containing 50 mL phosphate buffered saline (PBS) with pH values as 5.8 and 7.2, and the temperature was maintained at 37 °C. The whole process was performed in dark environment. At certain intervals (10 min, 20 min, 30 min, 50 min, 70 min, 1.5 h, 2 h, 2.5 h, 3.5 h, 5.5 h, 7.5 h, 15 h, 24 h), dialysis solution with 3 mL was drawn for concentration analysis of released LAM, and 3 mL corresponding PBS was added to maintain the constant volume. The absorbance of dialysate at 267 nm was measured by UV/Vis spectrophotometer, and LAM release at different pH values and times was calculated by the standard curve of LAM absorbance at 267 nm *versus* different LAM

concentrations. Finally, the cumulative release rate (CR) was calculated by the following formula:

$$CR\ (\%) = \frac{50.0C_n + 3.0\sum C_{n-1}}{W} * 100\%$$

where C_n and C_{n-1} represent the concentrations (μg mL^{-1}) of LAM in dialysate at the No. (n) and No. (n-1) sampling, W is the loaded amount of LAM (μg); n is the time of sample extraction.

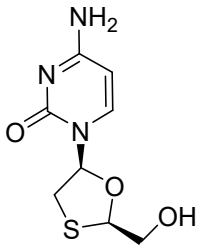

Figure S1. The chemical structure of lamivudine (LAM).

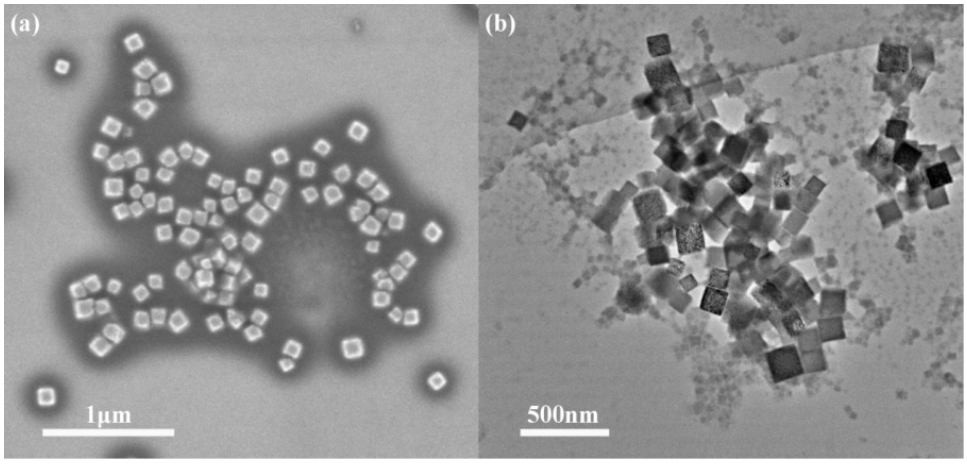

Figure S2. (a) SEM and (b) TEM images of **PB-S** nanoparticles.

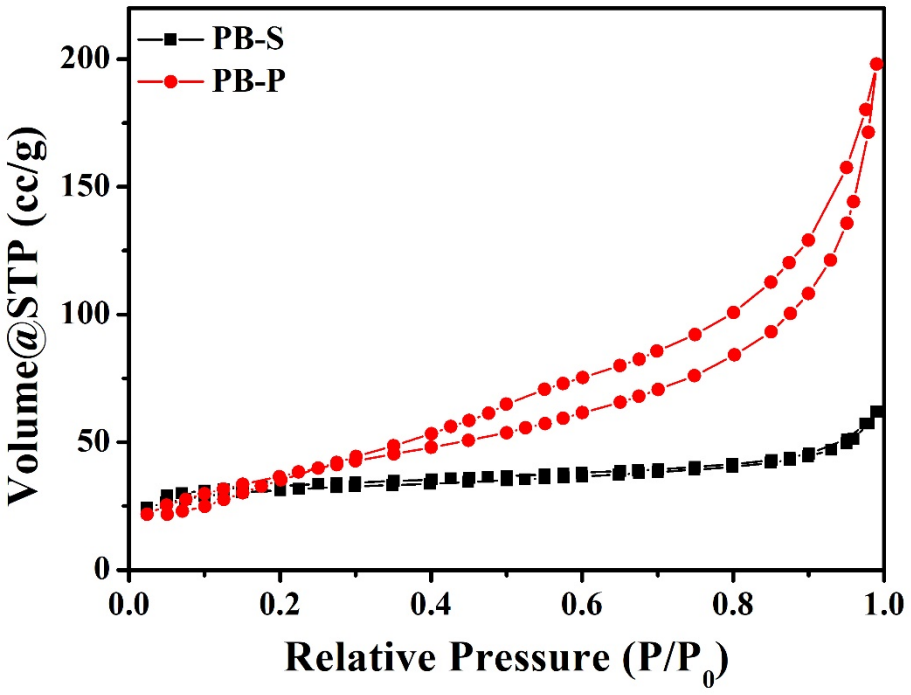

Figure S3. N_2 adsorption isotherms of **PB-S** and **PB-P** nanoparticles.

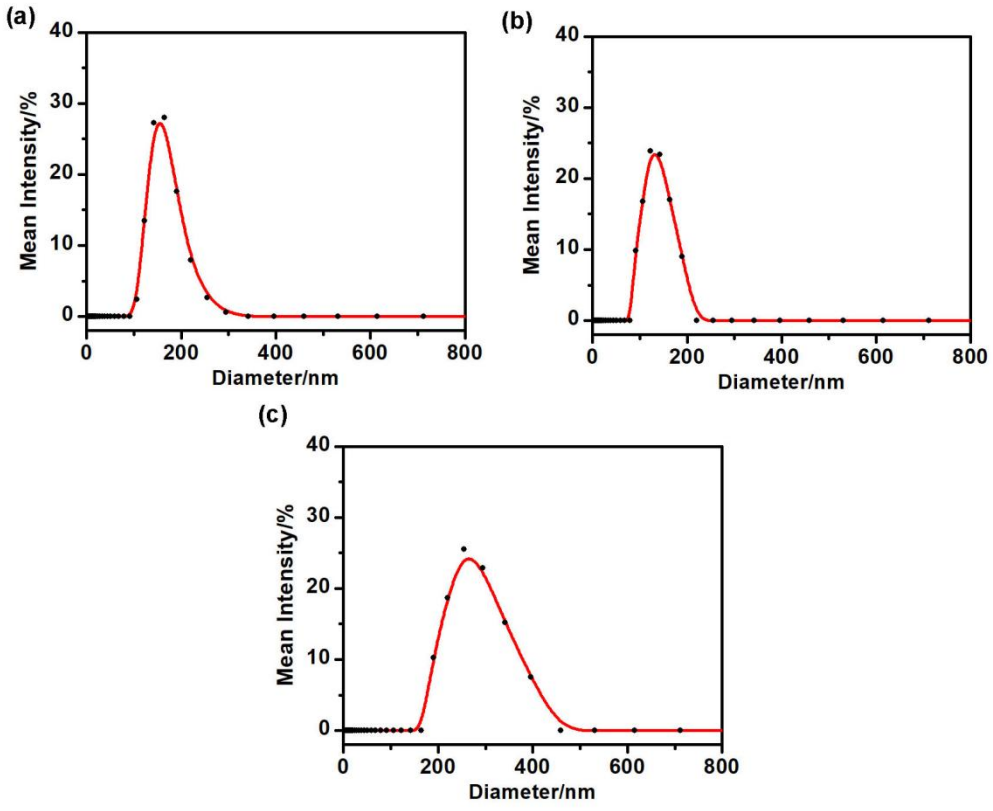

Figure S4. DLS results of (a) **PB-S**, (b) **PB-P**, and (c) **BSA@PB-P** nanoparticles.

The colloidal stability of **PB-P** and **BSA@PB-P** nanoparticles were measured in different aqueous media. As shown in **Figure S5**, **PB-P** and **BSA@PB-P** nanoparticles with 1 mg mL^{-1} were respectively dispersed in deionized water, phosphate buffered saline (PBS, pH = 7.2), Dulbecco's modified eagle medium (DMEM), and fetal bovine serum (FBS). After solution preparation, **PB-P** and **BSA@PB-P** nanoparticles presented uniform dispersion and satisfactory stability temporarily (**Figure S5a** and **S5c**). However, after centrifugation of 2567 g for 10 min, in **Figure S5b**, **PB-P** nanoparticles showed stability in water, but most of which sedimentated in PBS and DMEM, indicating the poor biocompatibility of **PB-P** in salt solution. Unexpectedly, PB-P exhibited good dispersity in FBS, which might be due to the adhesion of bovine serum onto the surface of **PB-P**, and improve the biocompatibility of obtained **FBS@PB-P** nanoparticles in FBS. As comparison, **BSA@PB-P** nanoparticles still presented well-distributed solution after centrifugation and no precipitation could be observed in solution (**Figure S5d**), which might be ascribed to the protection effect and biocompatibility of BSA shell in **BSA@PB-P** nanoparticles. In **Figure S5e**, after standing still for 7 days, most of **PB-P** nanoparticles were precipitated in DMEM, but **BSA@PB-P** nanoparticles maintained the colloidal stability in high salt DMEM solution with tiny precipitation due to the satisfactory biocompatibility nature of **BSA@PB-P** nanoparticles. In addition, we also performed DLS experiments to measure the particle sizes of **PB-P** and **BSA@PB-P** in PBS (pH = 7.2 and pH = 5.8) at 0 h and 24 h. As shown in **Figure S6**, the hydrodynamic diameters of **PB-P** in PBS at

pH = 7.2 and pH = 5.8 were measured as 139.0 nm and 136.8 nm, respectively, which were basically in accordance with the result of **PB-P** in aqueous solution (134.2 nm). However, after settlement for 24 h, the hydrodynamic diameters of **PB-P** increased to 187.1 nm and 178 nm, respectively, which indicated that **PB-P** had tendency of aggregation in PBS, which could precipitate after centrifugation as in **Figure S5**. For **BSA@PB-P**, the hydrodynamic diameters at pH = 7.2 and pH = 5.8 were 290.7 nm and 283.6 nm, and the corresponding data were almost unchanged as 281.6 nm and 274.2 nm after 24 h settlement, indicating that pH-dependent aggregation could not be observed in **BSA@PB-P**.

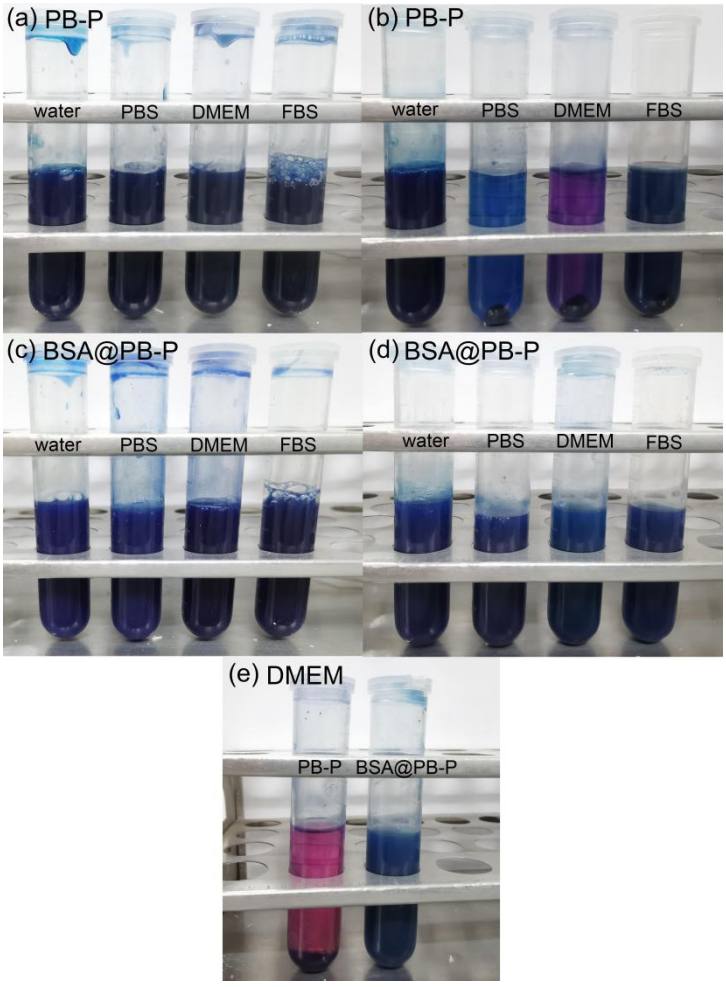

Figure S5. The colloidal stability of **PB-P** nanoparticles in water, PBS, DMEM, and

FBS (a) before and (b) after centrifugation of 2567 g for 10 min; the colloidal stability of **BSA@PB-P** nanoparticles in water, PBS, DMEM, and FBS (c) before and (d) after centrifugation of 2567 g for 10 min; (e) **PB-P** and **BSA@PB-P** nanoparticles in DMEM after standing still for 7 days.

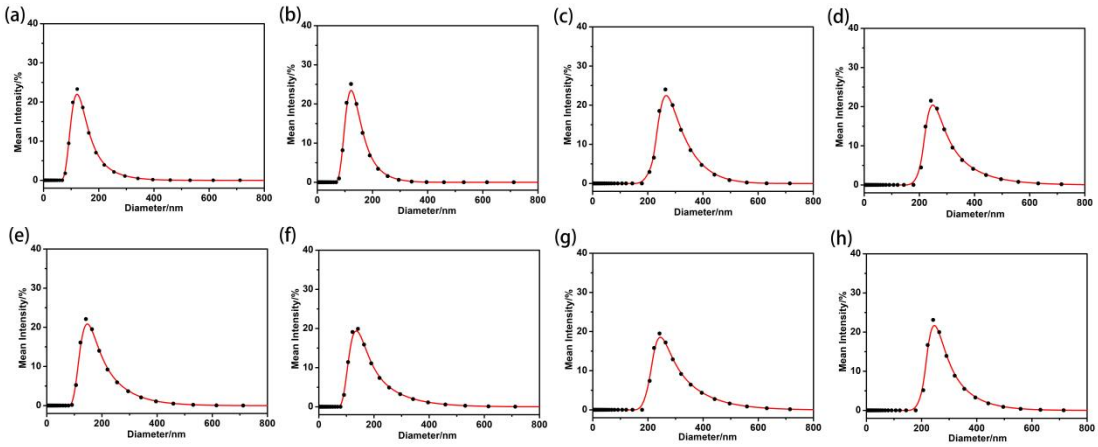

Figure S6. The DLS results of (a) **PB-P** in PBS (pH = 7.2), (b) **PB-P** in PBS (pH = 5.8), (c) **BSA@PB-P** in PBS (pH = 7.2), (d) **BSA@PB-P** in PBS (pH = 5.8), and corresponding results (e) (f) (g) (h) after settlement for 24 h.

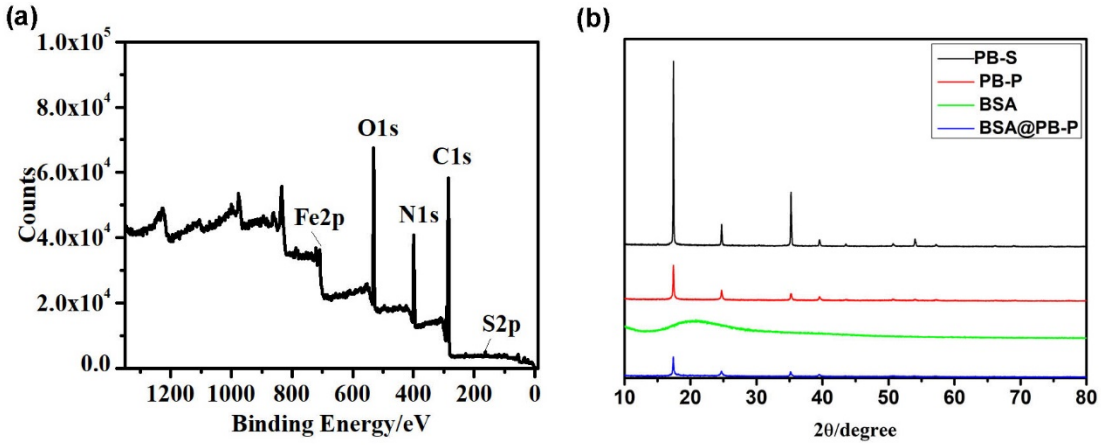

Figure S7. (a) The XPS result of **BSA@PB-P** nanoparticles, (b) the XRD results of **PB-S**, **PB-P**, BSA, and **BSA@PB-P** nanoparticles.

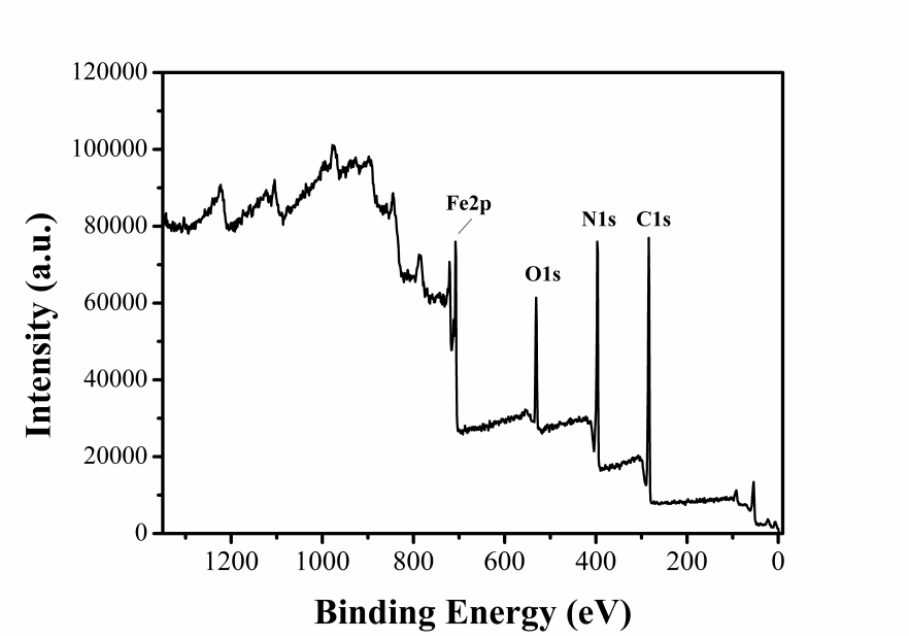

Figure S8. XPS spectrum of **PB-P** nanoparticle.

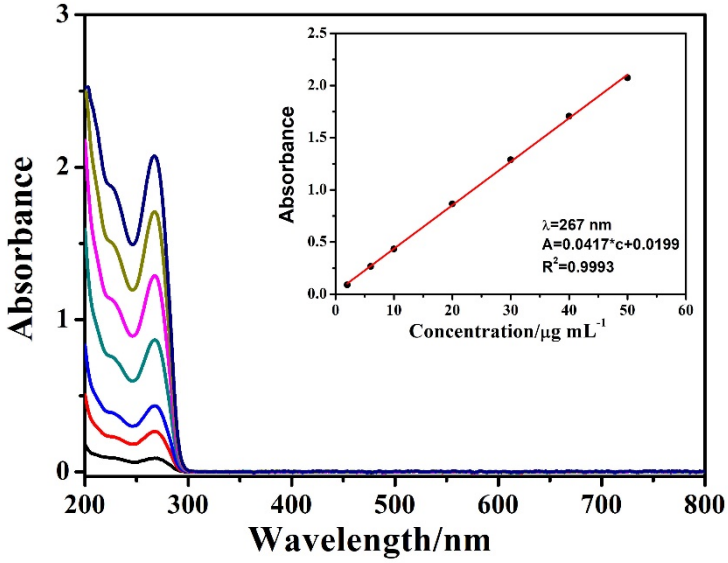

Figure S9. UV/Vis spectra of LAM with 2, 6, 10, 20, 30, 40, 50 μg mL^{-1} in aqueous solution. Inset: standard curve of absorbance *versus* LAM concentration at λ = 267 nm.

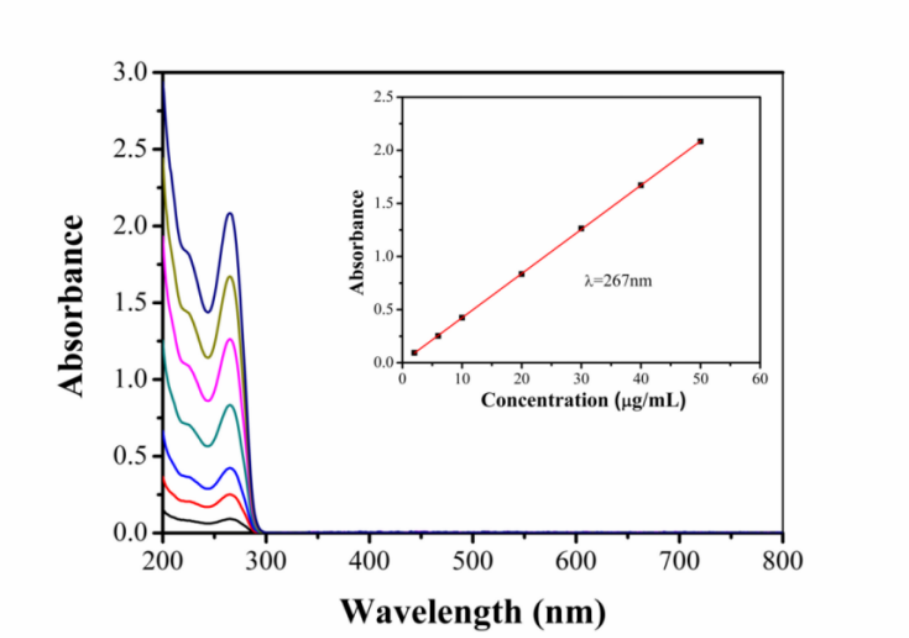

Figure S10. UV/Vis spectra of LAM with 2, 6, 10, 20, 30, 40, 50 μg mL^{-1} in PBS (pH = 7.2). Inset: standard curve of absorbance *versus* LAM concentration at λ = 267 nm.

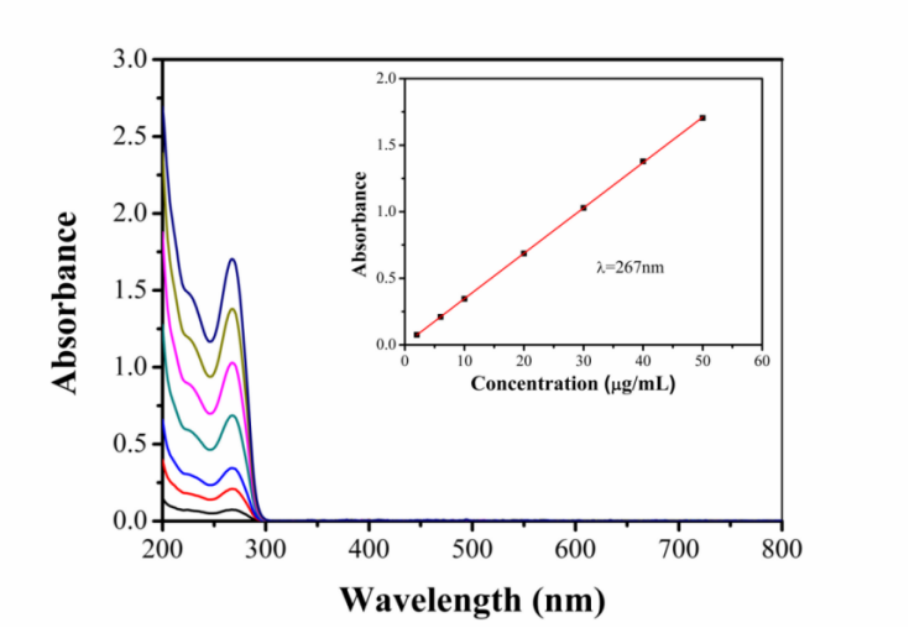

Figure S11. UV/Vis spectra of LAM with 2, 6, 10, 20, 30, 40, 50 μg mL^{-1} in PBS (pH = 5.8). Inset: standard curve of absorbance *versus* LAM concentration at λ = 267 nm.

Table S1. The loading rate of nanoPB with different etching time toward LAM (10 mg).

Etching time (h)	0	2	2.5	3
Loading rate (%)	11.36	17.45	35.73	-[a]

[a] The nanoPB after 3 h chemical etching is too trace mount to collection.

Table S2. BET analysis results of nanoMOFs.

	BET Surface Area (m^2 g^{-1})	Pore Volume (cm^3 g^{-1})	Adsorption Average Pore Width (nm)
PB-S	50.78	0.065	1.35
PB-P	239.92	0.347	3.93

Table S3. Surface element content of hierarchically porous **PB-P** nanoMOF.

Name	Fe2p	C1s	N1s	O1s
Atomic (%)	5.91	52.94	30.37	10.79

Table S4. Surface element content of **BSA@PB-P** nanoparticles.

Name	Fe2p	C1s	N1s	O1s	S2p
Atomic (%)	2.62	62.51	18.16	15.65	1.05

Table S5. The encapsulation rate and loading rate of **BSA@PB-S** toward LAM (4 mg, 6 mg, 8 mg, 10 mg, 12 mg).

LAM (mg)	4	6	8	10	12
Encapsulation rate (%)	6.43	8.08	8.26	7.34	6.57
Loading rate (%)	6.69	12.46	16.66	18.64	19.05

Reference:

[1] M. Hu, S. Furukawa, R. Ohtani, H. Sukegawa, Y. Nemoto, J. Reboul, S. Kitagawa, Y. Yamauchi, Synthesis of Prussian blue nanoparticles with a hollow interior by controlled chemical etching. *Angew. Chem. Int. Ed.* **2012**, *51*, 984-988.